

Propagation-Arrest in Structural Steel

Masao Yoshiki*
Takeshi Kanazawa*
and Susumu Machida*

Abstract:

Fracture mechanics developed by Dr. Irwin is applied to brittle fracture propagation-arrest problem. Results of Double Tension Test are newly interpreted from the viewpoint of fracture mechanics and it is assured by experimental and analytical researches using Double Tension Test specimen with patch or stiffener for crack arrester devices that the toughness for brittle fracture propagation-arrest can properly be grasped by material constant K_c (critical stress intensity factor for arrest).

1. Introduction

In Japan "Double Tension Test" is widely adopted as a largescale laboratory test to evaluate propagation-arrest characteristics of brittle fracture of steel plates. The test specimen and procedure are shown in Fig. 1. The results of this test have been expressed in terms of critical stress vs. temperature curve, which is directly utilized as design basis for determining the design stress and temperature of a given steel structure. This is based on rather intuitive consideration that it solely depends on the temperature and stress to which steel plate has been exposed prior to the appearance of brittle crack whether the crack will continue to propagate or not.

The authors applied fracture mechanics concept developed by Dr. Irwin to brittle fracture propagation-arrest problem and extended to the quantitative evaluation of toughness of steel for arresting of brittle crack.

Earlier, they applied this method in the clarification of the mechanism of brittle fracture propagation-arrest phenomenon of Double Tension Test and proposed a new interpretation for propagation-arrest characteristic instead of conventional critical stress-temperature curve which is not determined uniquely.¹ Lately Koshiga et al. have made further investigation on this problem.²

* Department of Naval Architecture, Faculty of Engineering, University of Tokyo, Japan.

In the serial research works the authors made approximate fracture mechanics considerations of the crack arresting mechanism; they concluded that the arresting phenomenon could be expected by the following criterion; a crack is arrested, if the stress intensity factor K is made smaller than the propagation resistance value K_c of the material as obtained, for example, from Double-Tension Test.^c In this report, they took up the patch type arrester as a fundamental model for the analysis of crack arresting mechanism and confirmed the above criterion on this model: in connection with afore-mentioned considerations brittle fracture propagation test using test specimens attached with crack arresting devices such as shown in Fig. 2. was carried out. Behaviors of brittle crack propagation were investigated by the analyses on the relation between calculated K -curve and K_c value obtained from Double Tension Test.

2. Analytical Considerations

A model as schematically shown in Fig. 3 is assumed, in which a semi-infinite plate subjected to a uniform tensile stress σ is attached with a rectangular patch with length ℓ and width b , said patch being joined only at its upper and lower ends to the plate. Owing to progressive development of a crack from an end of this plate, the patch acts as an arrester, that is, it restrains displacement of the plate through which the crack propagation of crack is resisted by the arresting action of the patch. With this simple, mechanical model, an approximate calculation with application of elasticity theory will be made to reveal how the so-called K -value of the crack propagation is affected by the patch dimensions and other factors.

In this model, with crack propagation, the plate is subjected to a compression P' (Pxt where t is thickness of patch) from the patch, while the patch is subjected to a tension P' , as its reaction. Thereby the magnitude and distribution pattern of P are supposed to depend on the crack length a , uniform tensile stress; dimensions of patch, its position and rigidity. But strict treatment of this problem would be considerably troublesome, so the elasticity solution of crack as evolved by Muskhelishvili³ using complex stress function will be exploited.

Erdogan et al.⁴ treated crack problems with the aid of Muskhelishvili's work and defining complex stress intensity factor combining its "symmetric" and "Skew symmetric" components, and discussed the method of its computation with the use of complex stress function.

The stress intensity factor K at crack tip ($a, 0$) in Fig. 4(a) can be obtained through relatively simple calculation using complex stress functions given by Muskhelishvili.

$$K = \frac{1}{2\pi\sqrt{a}} \left\{ R \left(\frac{J-1}{J+1} \right) + \frac{R}{J+1} \frac{a+z_0}{\sqrt{z_0^2-a^2}} - J \frac{a+z_0}{\sqrt{z_0^2-a^2}} + \left\{ \frac{\bar{R}(\bar{z}_0-z_0)}{J+1} + iM \right\} \frac{a}{(\bar{z}_0-a)\sqrt{z_0^2-a^2}} \right\} \quad (1)$$

$J = (3-\nu)/(1+\nu)$ ν : Poisson's ratio (for plane stress condition)

From eq. (1) K -value is found as following when concentrated forces in y -direction act symmetrically as illustrated in Fig. 4(b) (designated as K_p).

$$k_p = \frac{K_p/P\sqrt{x_0}}{\pi\sqrt{C}} = \frac{1}{\pi\sqrt{C}} \frac{1}{\sqrt{\rho_1\rho_2}} \left\{ (\rho_1+\rho_2) \sin\left(\frac{\theta_1-\theta_2}{2}\right) - \frac{2C\alpha}{J+1} \left\{ \frac{1}{\rho_1} \cos\left(\frac{3\theta_1+\theta_2}{2}\right) + \frac{1}{\rho_2} \cos\left(\frac{\theta_1+3\theta_2}{2}\right) \right\} \right\} \quad (2)$$

In eq. (2), P = concentrated force per unit plate thickness acting in y -axis positive direction at the first quadrant point $z_0(x_0, y_0)$.

$$z_0 = x_0 + iy_0, \quad r_1 = \sqrt{(x_0-a)^2 + y_0^2}, \quad r_2 = \sqrt{(x_0+a)^2 + y_0^2}$$

$$\theta_1 = \tan^{-1} \left\{ y_0/(x_0-a) \right\}, \quad \theta_2 = \tan^{-1} \left\{ y_0/(x_0+a) \right\}$$

$$a/x_0 = C, \quad r_1/x_0 = \rho_1, \quad r_2/x_0 = \rho_2, \quad r/x_0 = \rho, \quad y_0/x_0 = \alpha$$

Next, the case, as shown in Fig. 4(c), of point moments acting symmetrically can be expressed in the similar manner. Namely,

$$k_M = \frac{K_M}{M_t/x_0\sqrt{x_0}} = \frac{\sqrt{C}}{\pi\sqrt{\rho_1\rho_2}} \left\{ \frac{1}{\rho_1} \sin\left(\frac{3\theta_1+\theta_2}{2}\right) + \frac{1}{\rho_2} \sin\left(\frac{\theta_1+3\theta_2}{2}\right) \right\} \quad (3)$$

where M_t = moment in clockwise direction per unit plate thickness at first quadrant point $z_0(x_0, y_0)$.

The magnitude of stresses in the patch depends on the relation between the rigidity of cracked plate and the patch. In the case of the patch width being small, they can approximately be substituted by concentrated force. The force can be determined by the following condition for the continuation of displacement at patch ends:

$$V_0 = V_1 - V_2 \quad (4)$$

V_0 = vertical displacement at point (x_0, y_0) corresponding to patch end, as caused through uniform tensile stress in case of no patch.

V_1 = 1/2 elongation of patch due to tension P occurring in patch.

V_2 = displacement of patch end point in the plate through reaction to P .

V_0, V_1 and V are of course functions of crack length.

Now putting the tension in the patch as $P'(c)$ and the rigidity (spring-constant) of patch as m , we get

$$V_1 = \frac{1}{2} \frac{P'(c)}{m} \quad (5)$$

Meanwhile, the value of V_0 may be derived from the Westergaard stress function of elastic crack and can be calculated as follows:

$$V_0/\sigma_x = \sqrt{P_1 P_2} \left\{ 2 \sin\left(\frac{\theta_1 + \theta_2}{2}\right) - \frac{(1+\nu)\alpha P}{P_1 P_2} \cos\left(\theta - \frac{\theta_1 + \theta_2}{2}\right) \right\} - \nu \alpha \quad (6)$$

Further, the value of V_2 can be obtained from the "effective spring constant" of a crack-containing plate, namely the relation between the force P acting as in Fig. 4(b) and the displacement of its application point.

As is well-known, the effective spring constant M is related to K as follows:

$$G = -\frac{1}{2} (P')^2 \frac{dM}{M^2} = t \left(\frac{\pi}{E} K^2 da \right) \quad (7)$$

where t is plate thickness.

Integrating eq. (7), we have

$$\frac{(P')^2}{2} \left\{ \frac{1}{M} - \frac{1}{M_0} \right\} = \frac{\pi t}{E} \int_0^a K^2 da \quad (8)$$

where $P' = P \cdot t$, $K^2 = K^2(P/\sqrt{x_0})^2$ and $da = x_0 dc$ ($c = a/x_0$), namely,

$$\frac{1}{M(c)} = \frac{1}{M(0)} + \frac{2\pi}{E \cdot t} I(c) \quad (9)$$

where $I(c) = \int_0^c K^2 dc$.

The value of $M(c)$ is approximately calculated as follows with the use of elastic solution of the case where a concentrated force acting at a point in an infinite plate.

$$M(0) = \frac{1+\nu}{2\pi E t} \left\{ (3-\nu) \left(\ln \frac{\beta}{4\alpha} - 1 \right) + (1+\nu) \left(2 - \frac{1}{1+\alpha^2} \right) + (3-\nu) \ln \frac{1}{\sqrt{1+\alpha^2}} \right\} \quad (10)$$

where $\alpha = y_0/x_0$, $\beta = b/x_0$.

After $M(c)$ is found as in the above, we get

$$V_2 = \frac{2P'(c)}{M(c)} \quad (11)$$

where $2P'(c)$ represents the case of patches being attached on each side of the plate. Using eq. (4), $P'(c)$ is given by

$$P'(c) = V_0 / \left\{ \frac{2}{M(c)} - \frac{1}{m} \right\} \quad (12)$$

From this the value of P can be found and from eq. (2) the value of K_p can be calculated.

The above concerns the calculation of the tension $P'(c)$ acting in a patch with small width. When the patch has a large width, the effect of width should be taken into account. It would be difficult to make exact calculation of the distribution pattern in width direction of the stress in the patch, so an approximation is made by splitting as shown

in Fig. 5(a), the patch into several independent narrow elements. Thus, by finding the tensile force in each of these elements by the process described above, the distribution pattern of tensile stress in the patch may be approximately determined as Fig. 5(b).

If P in eq. (2) is substituted by the distributed force thus found and is integrated as to the patch width, K -value can be obtained. When, however, the patch width is not very large as compared with x_0 , the value may be further divided, as indicated in (c), into a tension component and a bending moment for the sake of simplicity. The value of K may then be calculated by the equation already given.

As for specimen with reverted stiffener, the effective rigidity of arresting element should be estimated. Once it is done, K value is calculated by the similar considerations for patch type arrester. Consider a system such as shown in Fig. 6(a) for an approximate calculation of effective rigidity of rivetted stiffener. System (a) could approximately be replaced by (b). As an approximation of the effect of width of stiffener b_p , a mechanical system in infinite plate such as shown in (c) is considered.

The relation between rivet force P' and displacement V is obtained as following after some calculations:

$$V = \frac{-P'(1+\nu)}{4\pi E t_p} \left\{ (5-3\nu) + (3-\nu) \ln \sqrt{1 - \left(\frac{r}{l}\right)^2} + 2(1-\nu) \sum_{j=1}^{\infty} (-1)^j \frac{1}{2j+1} \left(\frac{r}{l}\right)^{2j} + 2 \sum_{n=1}^{\infty} \left\{ (3-\nu) + \frac{3-\nu}{2} \ln \frac{(nb_p)^2 - r^2}{\{(nb_p)^2 + l^2 + r^2\}(1-4A_n^2)} \right\} \frac{1}{2j+1} \left(\frac{r}{l}\right)^{2j} + \sum_{j=1}^{\infty} \frac{1}{2j+1} \left\{ \left(\frac{r}{nb_p}\right)^{2j} - (3-\nu) \frac{nb_p}{r} A_n^{2j+1} - (5-3\nu)(-1)^j \frac{r}{l} B_n^{2j+1} \right\} \right\} \quad (13)$$

where $r = Dr/2 =$ radius of rivet hole
 $t_p =$ plate thickness of stiffener
 $b_p =$ width of stiffener
 $l =$ pitch of rivets
 $A_n = \frac{nb_p r}{(nb_p)^2 + l^2 + r^2}$
 $B_n = \frac{lr}{(nb_p)^2 + l^2 - r^2}$

3. Experiment

Chemical compositions, tensile test properties and brittle fracture propagation-arrest characteristics (K_c vs. temperature relation) obtained from Double Tension Test of test steels are shown in Table 1 and Fig. 7.

Specimens used are shown already in Fig. 2, which are Double Tension Test Specimens with arresting elements (patch type and rivetted stiffener type) attached to their central portion. The dimensions of arresting elements are varied which are given Table 2.

Most of specimens with welded patch were annealed at 600 C x 2 hours in order to remove welding residual stress but three out of five GWT specimens were tested at as welded condition. The magnitude of welding residual stress was measured by P fender's contact ball type strain meter.

Summarized results of test are also tabulated in Table 2. Fracture mechanics analyses were made on each of specimens and some examples of them are presented graphically in the form of K curves and K_C curves vs. crack length in Fig. 8. K curves were calculated by the method described in the foregoing sections. K_C curves were illustrated using the $K_C - T$ relations shown in Fig. 7 in accordance with the given temperature distributions with the allowance of $\pm 10\%$ scattering band, which is shown by hatching.

From these Figures it can generally be said that a brittle crack is arrested if the K value of the system considered is made smaller than the K_C value of the material due to the arresting effect of patch or riveted stiffener and it can endure the reaction of arresting forces.

In Fig. 9, K values at arrest point of the specimen with arresting element (marks with arrow represent minimum value of K in case where brittle crack propagated through) are plotted against temperature scale, which shows good agreement with those obtained from Double Tension Test.

On the K curves calculated stresses occurred in the patch or rivet (shear stress) are indicated for the explanation of the test result of the specimen the arresting element of which was broken and the brittle crack ran through.

It can generally be concluded that the brittle fracture propagation-arrest phenomenon can be explained by relatively simple calculation based on fracture mechanics.

4. Conclusion

With the application of two dimensional elasticity theory of cracked plate, fracture mechanics analyses were made on the simple models for patch and riveted stiffener type of crack arrester, and experimental checks were made by conducting Double Tension Test using specimens with those arresting elements.

Approximate calculations and experiments executed in this report showed the adequacy of simple criterion for brittle fracture propagation-arrest based on fracture mechanics.

References

1. M. Yoshiki, T. Kanazawa & S. Machida, Proc. the 7th Japan Congress on Testing Materials, March, 1964.
2. F. Koshiga, IIW Doc. IX-412-64 or X-334-64, January, 1964.
3. I.N. Muskhelishvili: "Some Basic Problems of Mathematical Theory of Elasticity", Noordhoff Ltd., Groningen-Netherlands, 1963.
4. F. Erdogan, Proc. the 4th U.S. Congress of Appl. Mech.

Table 1 Chemical Composition and Tensile Properties of Test Steel

Code	Type of Steel	Chemical Composition (Ladle) (%)									
		C	Si	Mn	P	S	Ni	Cr	Mo	Al	
AK	Al-Killed	0.10	0.25	1.27	0.014	0.012	0.17	0.04	0.05	0.028	
GWT-5	50kg/mm ² Class High Strength Steel(as roll)	0.16	0.44	1.37	0.022	0.012				0.014	

Tensile Test Properties			
Code	Yield Stress (Kg/mm ²)	Tensile Strength (Kg/mm ²)	Elongation G.L.=50mm (%)
AK	41	50	52
GWT-5	36	58	27

Table 2(a) SUMMARY OF TEST RESULTS OF DOUBLE TENSION SPECIMEN WITH WELDED PATCH ARRESTER

Specimen code	Test Plate t=20mm	Dimensions of patch			Welding residual stress	Test stress (Kg/mm ²)	Test temp T(°C)	Crack length a(mm)	Kc(Kg/mm ² -mm) estimation & Remark
		l _p (mm)	b _p (mm)	t _p (mm)					
AKP-1-10	AK	100	60	13	SR*	20	-47	60	Weld of patch was sheared
AKP-1-15	AK	150	60	13	SR*	16	-44	260	Kc = 164 at -44°C
AKP-1-20	AK	200	60	13	SR*	16	-46	--	Kc 172 at -46°C Initiation part was fractured
AKP-8	AK	150	80	13	SR*	16	-54	275	Kc = 108 at -54°C
AKP-2-15	AK	150	60	20	SR*	20	-46	264	KC = 140
AKP-2-20	AK	200	60	20	SR*	20	-49(-45)	425	G0 ? Kc ≤ 148 at -49°C
AKP-2-25	AK	250	60	20	SR*	20	-45	454	G0 ? Kc ≤ 184 at -45°C
GWT-5-2	GWT-5	100	60	10	SR*	15	-10	410	G0 ? Kc ≤ 100 at -10°C
GWT-5-4	GWT-5	150	60	10	SR*	15	0	285	Kc = 160 at 0°C
GWT-5-8	GWT-8	100	60	10	as weld	15	0 (-2)	200	Kc = 152 at -2°C
GWT-5-11	GWT-5	100	60	10	as weld	15	-10	60	weld of patch was sheared
GWT-5-7	GWT-5	150	60	10	as weld	10	-11	225	Kc = 75 at -11°C

* SR -- 600 C°x2hr. stress relief annealing
 ** Temperature at arrest point

Table 2(b) SUMMARY OF TEST RESULTS OF DOUBLE TENSION SPECIMEN WITH RIVETED ARRESTER (Test plate AK t=20mm

Specimen code	Dimensions of arrester			Diameter of rivet hole Dr (mm)	Test stress (Kg/mm ²)	Test temp T (°C)	Crack length a (mm)	Kc (Kg/mm ² ·mm) estimation & Remark
	l (mm)	b _p (mm)	t _p (mm)					
AKPR-4-10	100	40	13	20x1	16	-46	60	One of rivets was sheared Kc ≤ 212 at -46°C
AKPR-4-15	150	40	13	20x1	16	-46	60	One of rivets was sheared Kc ≤ 164 at -46°C
AKPR-8-10	100	80	13	17x2	16	-42(-51) (75)		Initiation Part was fractured Kc ≤ 132 at -51°C
AKPR-8-15	150	80	13	17x2	16	-46	265	Kc = 112 at -46°C
AKPR-8-20	200	80	13	17x2	16	-45	450	GO ? Kc 152 at -45°C

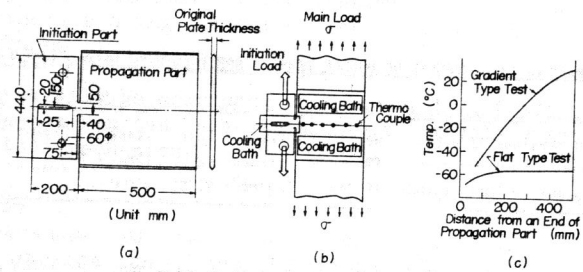


Fig. 1. Double Tension Test.
(a) Test Specimen.
(b) Test Procedure.
(c) Example of Temperature Distribution.

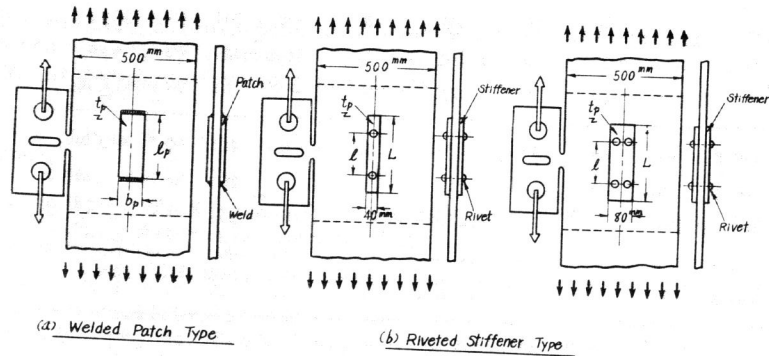


Fig. 2.

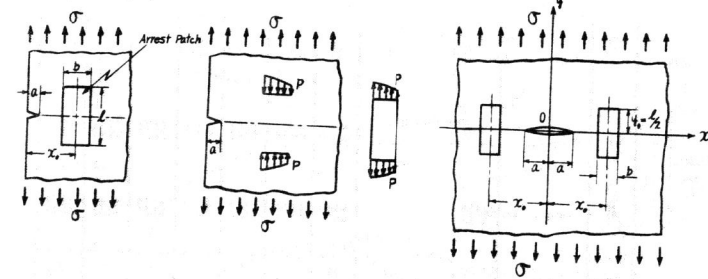


Fig. 3

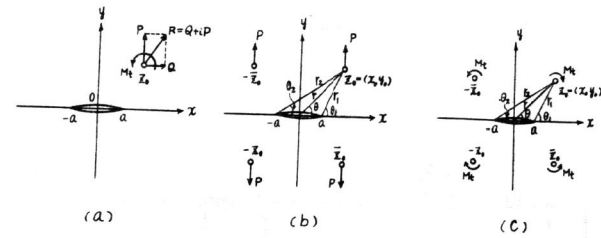


Fig. 4

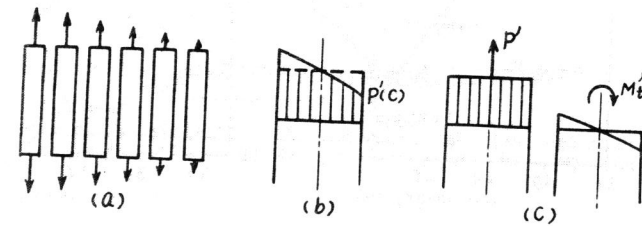


Fig. 5

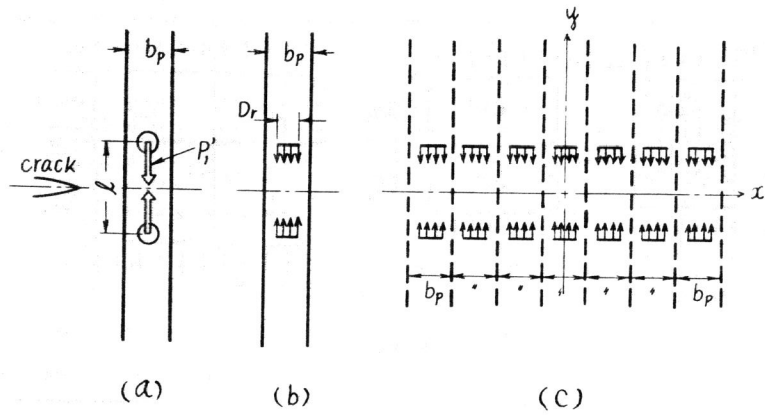


Fig. 6

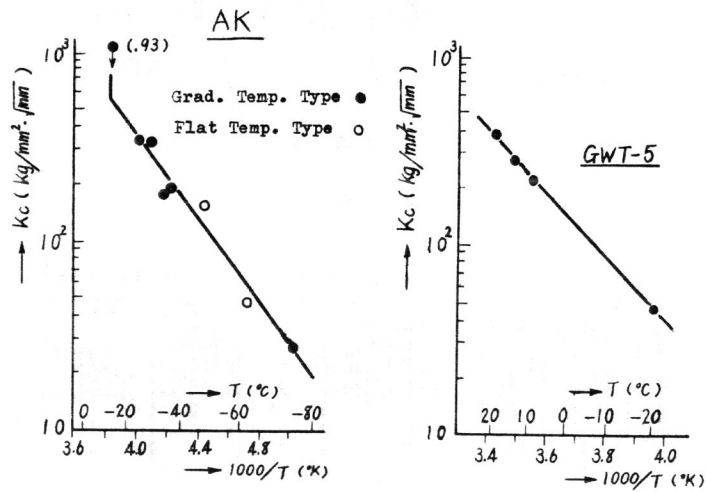
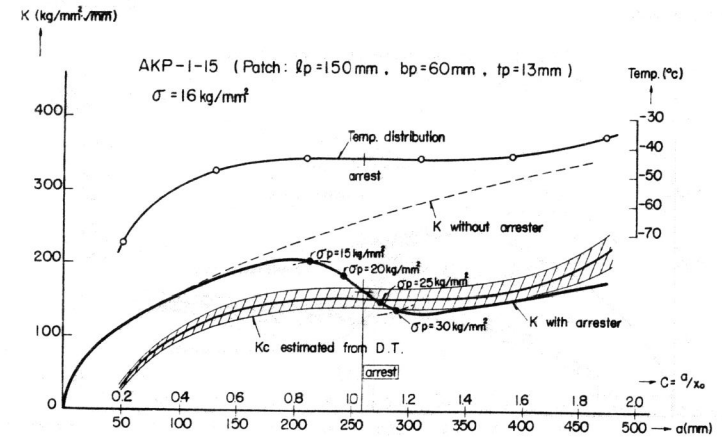
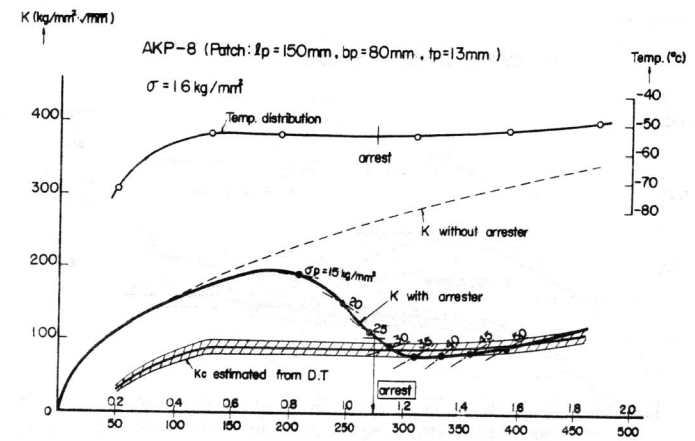


Fig. 7

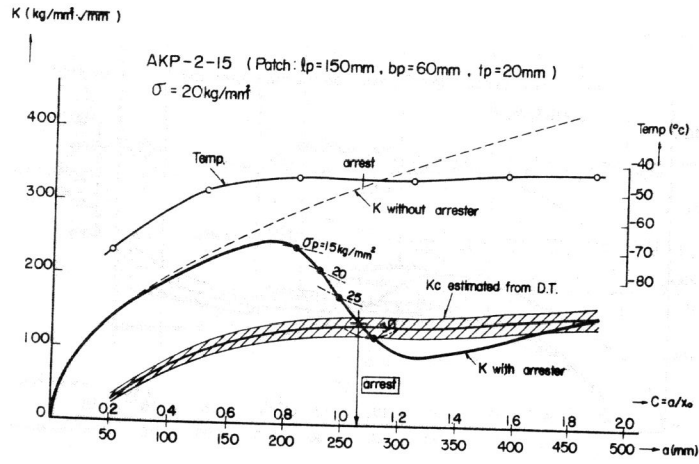


(a)

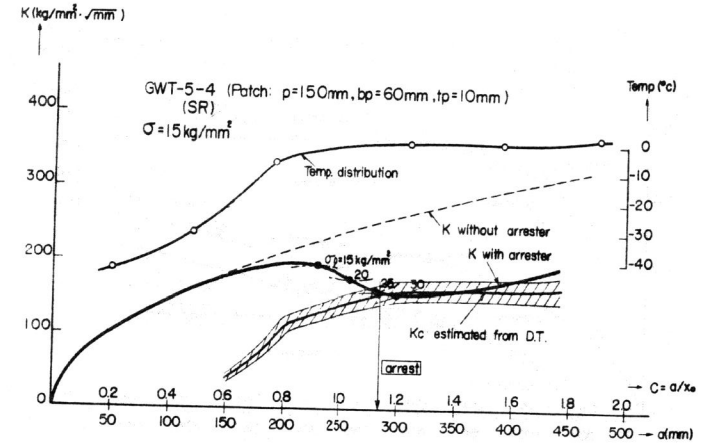


(b)

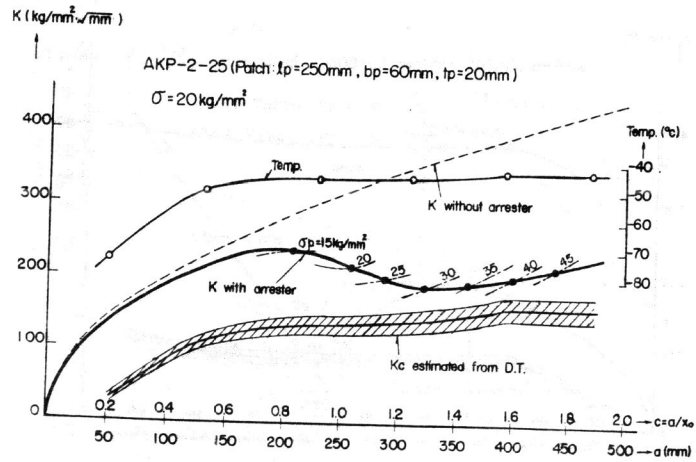
Fig. 8



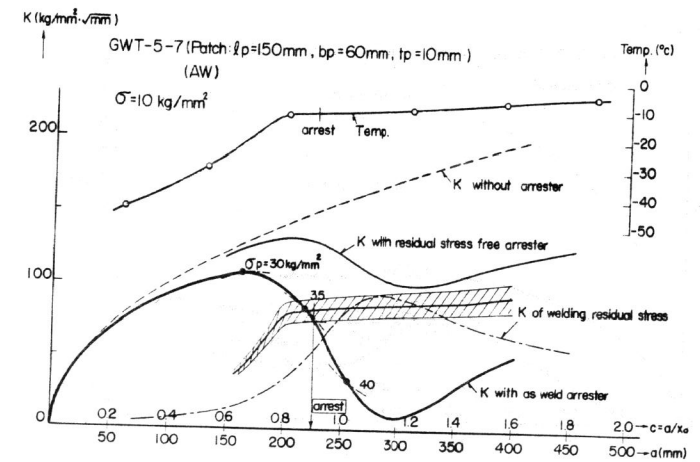
(c)



(a)



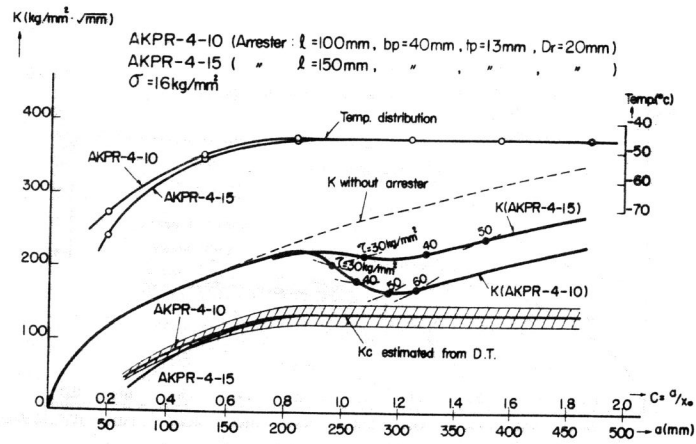
(d)



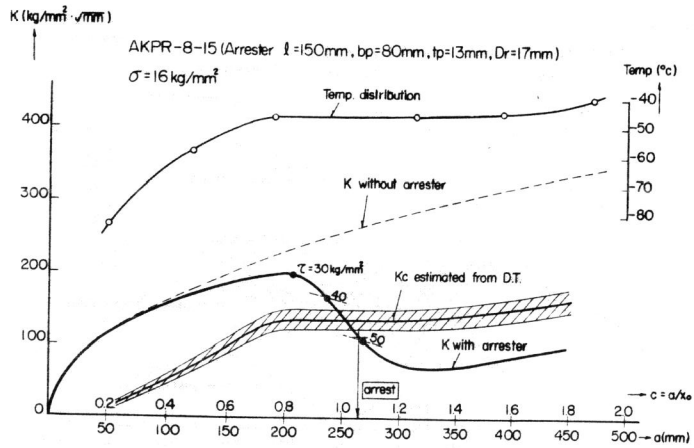
(f)

Fig. 8²

Fig. 8³

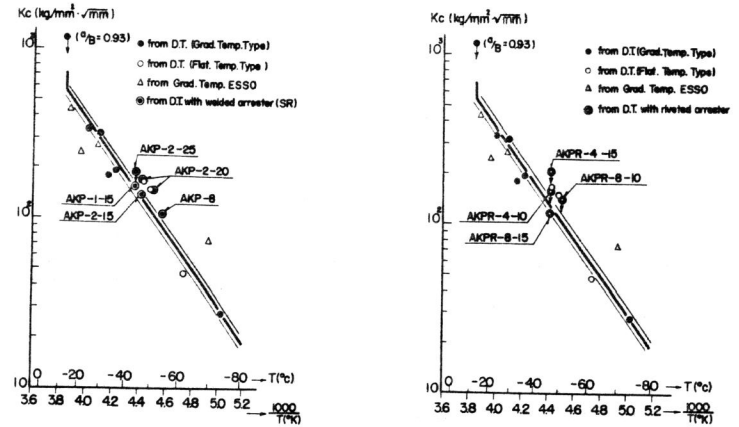


(g)

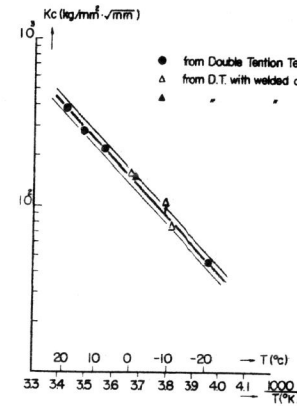


(h)

Fig. 8⁴



Kc~T: Test plate AK(AI killed)



Kc~T: Test plate GWT5 (HT55)

Fig. 9